JOURNAL OF SPACECRAFT AND ROCKETS
Vol. 42, No. 5, September–October 2005

Stabilization of Blunt Nose Cavity Flows by Using Energy Deposition

Leonid A. Bazyma*
National Aerospace University "Kharkov Aviation Institute," 61070 Kharkov, Ukraine
and
Vasyl M. Rashkovan†
National Polytechnic Institute, 04430 Mexico, D.F., Mexico

A computational investigation of the deposited energy per unit mass influence on the supersonic flow stabilization and the change of aerodynamic drag of the hemisphere with cylindrical cavity is presented. The results obtained suggest that pulsed sources of thermal flux would be an effective means of influencing the pulsating process during flow around cavity bodies.

Nomenclature

a	=	sound velocity
C	=	average drag coefficient
C_0	=	drag coefficient without the energy deposition
e	=	total energy per unit mass
f	=	pulse frequency
K	=	safety factor (similar in meaning to the Courant number)
k_1, k_2	=	constants, which define thermal spot shape
L	=	constant, which defines thermal spot shape
l_{cav}	=	depth of the cavity
M	=	Mach number
N	=	maximum pulse number
p	=	pressure
R	=	sphere radius
r_{cav}	=	cavity radius
Sr	=	Strouhal number
s	=	axial distance from the cavity base to the mean shock position
t	=	time
u, v	=	velocity vector components on the axes x and r
W	=	deposited energy per unit mass
W_0	=	constant, which defines deposited energy density
x, r	=	cylindrical coordinate system components
x_0	=	constant, which defines thermal spot shape
γ	=	ratio of specific heats
δ	=	Dirac delta function
ρ	=	density

Introduction

SUPERSONIC and hypersonic space vehicles are extremely sensitive to aerodynamic resistance. The combination of the two main rocket operation factors, low altitude and high velocity, produces considerable heat flows in the stagnation region of the nose. For this reason, passive heat-transfer analysis under such conditions is very important for understanding and solving rocket operation problems.

Recent analyses have shown that the nose-tip heat transfer can be reduced using a forward-facing nose-tip cavity[1–4] with minimal drag penalties. Additionally, coaxially directed optical sensors can be installed in the bottom of these cavities.[1,5] Such a forward-facing cavity concept has been the focus of some recent high-speed missile programs, including the hollow-nosed active seeker program and the hit-to-kill endoatmospheric strapdown seeker.[6]

It is well known that supersonic flow around bodies with cavities located on the nose is accompanied by pulsation.[7–9] A forward-facing cavity can be regarded as a resonance tube. One of the characteristics of a hollow-nosed missile at supersonic Mach number is an oscillating bow shock that can significantly influence missile drag, heat transfer, and optical signal propagation through the cavity.[1] Several methods of the bow shock stabilization have been considered. For example, the cavity can be gas pressurized in order to maintain a stable pressure and reduce the amplitude of shock oscillations in front of the cavity produced by movement of the bow shock.[10]

Flow stabilization by jet injection from the cavity bottom is discussed in previous work.[9] Control and manipulation of the pulsation process by energy deposition caused by the influence of a pulse laser is considered as well.[11–13]

The use of a laser to supply energy has been experimentally shown to be a good approach for both general and local flow control. Experimental research[11–12] shows that an extensive region of energy supply is realized in the supersonic flow when a powerful optical pulsating discharge is applied, with a thermal wake developing behind the area where the energy is supplied.

A cone or hemisphere in the thermal wake, located from 1.0 to 4.0 distance diameters from the focal plane of irradiation from a CO_2 laser, results in a reduction of aerodynamic drag of over a factor of two when a 100-kHz pulse frequency[12] is applied. The thermal wake becomes continuous[12] for 10–100-kHz radiation pulses.

Theoretical modeling results of the influence of a heat-release pulsating source on the supersonic flowing around the hemisphere are presented in Ref. 13. The explicit total-variation-diminishing (TVD) method in Chakravarthy's[14,15] formulation is applied in these calculations.[13] In the case of $M = 3$, $\gamma = 1.4$, and a constant deposited energy per unit mass, the aerodynamic load upon the body exhibited a decrease. A pulse repetition rate corresponded to a minimum drag was determined, and it was concluded that the use pulsating energy supply might be more effective than a constant energy source.

Other results[11–13,16] show that pulse repetition rate, the power supplied to the flow, and the area into which this energy is supplied all greatly influence both the pressure distribution and the model surface and its flow regimes. However, these results only considered hemispherical nose tips. The current work addresses the

Received 12 July 2004; revision received 19 November 2004; accepted for publication 14 December 2004.

*Associate Professor, Department 402, 17 Chkalov Street; bazima@htsc.kipt.kharkov.ua.

†Professor, National Aerospace University of Ukraine; also Professor-Invitee, High-School of Mechanics and Electric Engineer, Col. San Francisco Culhuacán, Av. Santa Ana No. 1000, Mexico; vasyl@calmecac.esimecu.ipn.mx.

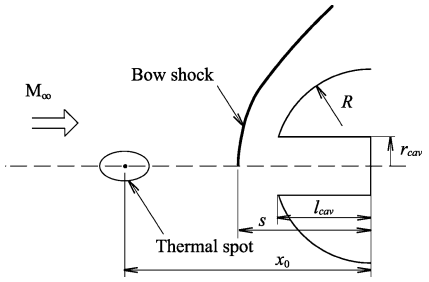

Fig. 1 Schematic of forward-facing cavity.

influence of the deposited energy per unit mass on the supersonic flow stabilization and the aerodynamic resistance changes of the hemisphere with a cylindrical cavity. The results from this work show that a heat-release pulsating source can be used as an effective supersonic flow control method for space vehicles with forward-facing cavities.

Problem Definition

Consider the problem of constant, quasiperiodic, axisymmetric flow around a hemisphere cylindrical cavity ($r_{cav}/R = 0.3$; $l_{cav}/R = 0.954$; $l_{cav}/r_{cav} = 3.18$) with a uniform, ideal supersonic gas flow. The forward-facing cavity scheme is depicted in Fig. 1. Assume that at time $t = 0$, a pulsating power supply source is initiated in front of the sphere.

The equations of gas dynamics in the cylindrical coordinates have the form

$$\frac{\partial \rho r}{\partial t} + \frac{\partial \rho u r}{\partial x} + \frac{\partial \rho v r}{\partial r} = 0 \tag{1}$$

$$\frac{\partial \rho u r}{\partial t} + \frac{\partial (p + \rho u^2) r}{\partial x} + \frac{\partial \rho u v r}{\partial r} = 0 \tag{2}$$

$$\frac{\partial \rho v r}{\partial t} + \frac{\partial \rho u v r}{\partial x} + \frac{\partial (p + \rho v^2) r}{\partial r} = p \tag{3}$$

$$\frac{\partial \rho e r}{\partial t} + \frac{\partial \rho u (e + p/\rho) r}{\partial x} + \frac{\partial \rho v (e + p/\rho) r}{\partial r} = \rho q r \tag{4}$$

Equation (1–4) involves the system variables, where q is the energy supplied from the external source per unit mass of the gas. The preceding system of equations is closed by the equation of state of the ideal gas

$$p = (\gamma - 1)\rho e \tag{5}$$

The energy supply q was described in a similar form as in Ref. 13:

$$q = W(x, r) \sum_{n=1}^{N} \frac{1}{f} \delta(t - t_n) \tag{6}$$

where N is the maximum pulse number ($N \gg 1$) and W is the average deposited energy per unit mass, which was chosen with some changes to model different thermal spot shapes

$$W = W_0 (p_\infty/\rho_\infty)^{\frac{3}{2}} (1/R) \exp\left\{-\left[k_1 r^2 + k_2 (x - x_0)^2\right] \Big/ L^2\right\} \tag{7}$$

where W_0, k_1, k_2, x_0, and L are some constants, which define deposited energy density and thermal spot shape.

Numerical Method

Equation system (1–4) solution was conducted by Godunov's method[17] on a 110×60 grid mesh, which was designed by densening the mesh point all around the body region, with the exception that in the cavity the mesh points distribution were set to be uniform. The calculations were performed using the same finite difference scheme of the first-order approximation as that employed in Ref. 17.

Grids used in calculations are shown in Fig. 2.

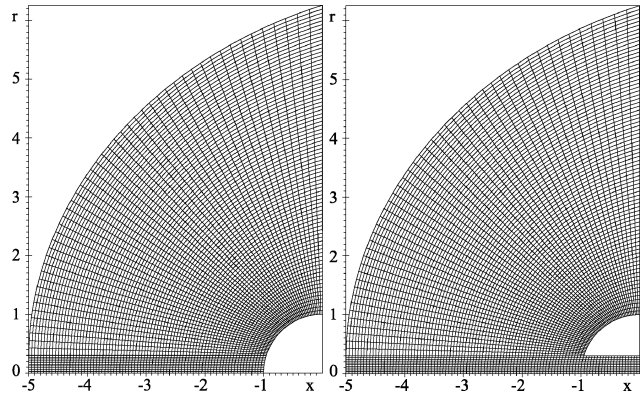

Fig. 2 Computational grid: a) for hemisphere and b) for cavity hemisphere.

The necessary and sufficient condition for stability is that the permissible spacing in time τ must satisfy the inequality

$$\tau/\tau_x + \tau/\tau_y \le 1 \tag{8}$$

that results from a stability study of Godunov's difference scheme realized on the system of nonstationary acoustic equations on a uniform rectangular (or parallelogram) grid. Here τ_x, τ_y are the time spacing of the one-dimensional scheme. Physically τ_x and τ_y are mean time intervals, in which waves that appear at the break decomposition on the cell boundary reach the neighboring boundaries:

$$\tau_x = \frac{\Delta x}{\max(u + a, a - u)}, \qquad \tau_y = \frac{\Delta y}{\max(v + a, a - v)} \tag{9}$$

The stability condition so given is extended to the quasilinear equations of gas dynamics. Calculations show that this condition (8) provides the necessary stability. Nevertheless, this condition is usually used with a right-hand side less than one.

In the current work, the time step is chosen from cell to cell according to the stability condition as follows:

$$\tau_{n-\frac{1}{2}, m-\frac{1}{2}} = [\tau_x \tau_r/(\tau_x + \tau_r)]_{n-\frac{1}{2}, m-\frac{1}{2}}, \qquad \bar{\tau} = \min_{n.m} \tau_{n-\frac{1}{2}, m-\frac{1}{2}} \tag{10}$$

In k space its value with respect to time is calculated by using the following spacing $k + 1$:

$$\tau^{k+1} = K \bar{\tau}^k \tag{11}$$

To use dimensionless values, we make use of the following equalities:

$$r = \bar{r} R, \qquad x = \bar{x} R, \qquad t = \bar{t} R/a_\infty, \qquad f = \bar{f} a_\infty / R$$

$$a = \bar{a} a_\infty, \qquad u = \bar{u} a_\infty, \qquad v = \bar{v} a_\infty, \qquad \rho = \bar{\rho} \rho_\infty$$

$$p = \bar{p} \rho_\infty a_\infty^2, \qquad W = \bar{W} a_\infty^3 \Big/ R \tag{12}$$

where a_∞ is the incident flow sound velocity. In the following text, we have omitted bars above the dimensionless values r, x, t, f, a, u, v, ρ, p, and W.

On the body surface and along the symmetry axis, solid-wall inviscid boundary conditions were applied. Along the external inflow boundary, undisturbed freesteam conditions were utilized. On the downstream outflow boundary, extrapolation of the flow quantities from the adjacent internal boundary was performed.

The initial data in calculations without energy deposition corresponded to the dimensionless parameters of the incident stream:

$$p = p_\infty = 1/\gamma, \qquad \rho = \rho_\infty = 1$$

$$u = u_\infty = M_\infty, \qquad v = 0 \tag{13}$$

Subsequent solutions of the cavity flow with energy deposition were initialized using the cavity flow solution without energy deposition. The solutions were advanced in time until the average flow conditions were stabilized.

Preliminary supersonic flow calculations around the cavityless hemisphere were conducted to confirm the adequacy our numerical scheme. Data reported in Ref. 13, where the explicit TVD method of Chakravarthy's formulation[14,15] was used, showed good correspondence in all of the observed flow regimes.

Shown in Fig. 3 is the dependence on the dimensionless time at pulse repetition rate $f = 0.5$, of the pressure at the stagnation point while flowing around the hemisphere (for $M_\infty = 3, \gamma = 1.4$). Results are shown both from Ref. 13 (Fig. 3a) and from the present work (Fig. 3b). One can see that the main pulsation parameters (period, amplitude) and their character obtained in this work correspond well to the data Ref. 13. The resolution of the numerical scheme used in Ref. 13 is somewhat higher. However, the scheme used in the present work allows us to obtain the quasi-stationary pulsation process.

Shown in Fig. 4a is the flow visualization near the hemisphere under the influence of the pulsating thermal source (spherical heat spot; $W_0 = 20$, $x_0 = -3.5$, $L = 0.5$). These results were obtained in Ref. 13 and compared with the analogous data of the present work (Fig. 4b). One can see from this figure that bow shock wave standoff distance, formed recirculation zones, and the flow in general, reported in Ref. 13 and the present work, are in good agreement.

The grid-resolution study was also conducted. The test calculations of both hemisphere and cavity hemisphere were done on the grid 219×119 for this purpose. The grid 219×119 was obtained through twice grid 110×60 spacing reduction. Minimum surface cell spacing was 0.024 for the grid 110×60 (reduced to the sphere radius) and 0.012 for the grid 219×119.

Figure 3b demonstrates solution comparison obtained by use of the grids 110×60 (the continuous line) and 219×119 (the dotted line). Obviously, the grid 219×119 resolution is higher than the grid 110×60 one. The solution obtained on the grid 219×119 marked out some peculiarities of pressure change on the compression stage. These peculiarities correspond to the solution in Ref. 13 too, but they were not seen through the grid applied. Solution difference obtained on the grids 110×60 and 219×119 is rather small for the hemisphere with energy deposition.

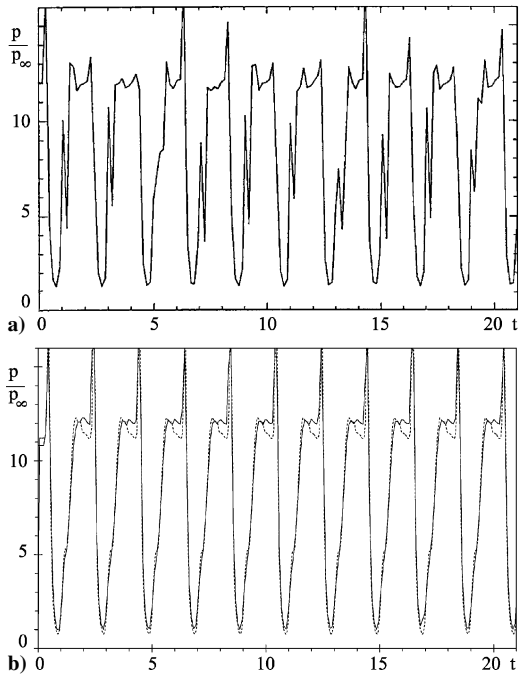

Fig. 3 Pressure dependence in the hemisphere stagnation point on the dimensionless time at the pulse repetition rate $f = 0.5$ (spherical heat spot; $W_0 = 20$, $x_0 = -3.5$, $L = 0.5$): a) results of Ref. 13 and b) present work (——, 110 × 60 grid; - - - -, 219 × 119 grid).

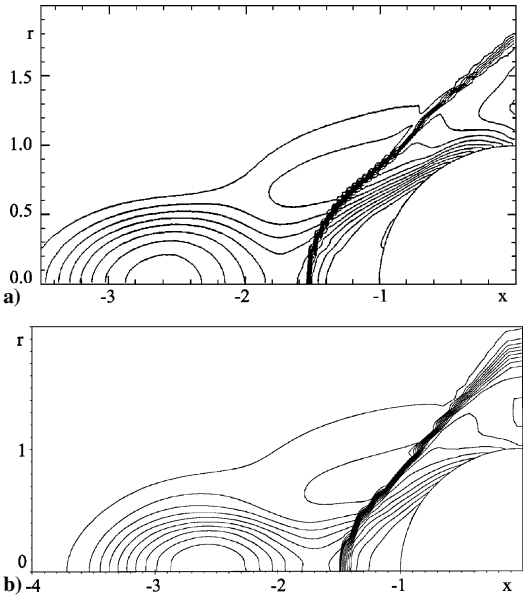

Fig. 4 Mach-number isolines while flowing around the hemisphere with supersonic gas flow at pulse repetition rate $f = 2$ ($t = 11.2$): a) results of Ref. 13 and b) present work.

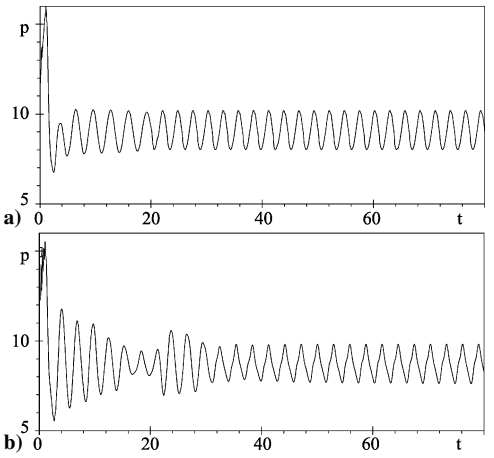

Fig. 5 Pressure variation in the center of the cavity bottom without energy deposition: a) 110 × 60 grid and b) 219 × 119 grid.

The cavity flow solution without energy deposition made using the grid 110×60 is presented in Fig. 5a. This solution accords well to the solution obtained using the grid 219×119 (Fig. 5b).

The details of the numerical scheme, along with test examples, are given in Refs. 17 and 18.

Results and Discussion

Predictions of the flowfield about a hemisphere with a forward-facing cavity were obtained for a freestream Mach number of 3 with and without energy deposition. For the cases with energy deposition, the supplied energy was modeled using Eqs. (6) and (7) with $x_0 = -3.5$, $L = 0.5$, $N = 100f$, and $t_n = n/f$ for $1 \le f \le 5$. Two thermal spot shapes were considered: a spherical shape ($k_1 = k_2 = 1$) and an ellipsoidal shape ($k_1 = 4$, $k_2 = 1$). The intensity of the energy deposition was varied; $20 \le W_0 \le 500$.

The time variation of the pressure at the center of the cavity bottom is presented in Fig. 6. The pulsation character (curve 1) and the Strouhal number $Sr = 0.245$ are close to the computational data[9] ($Sr = s/a_0 t^0$, t^0 is the oscillation period and a_0 sound velocity at the stagnation temperature). The pressure variation in the center of the cavity bottom is also observed in the experiments,[2,4,] where the flow around a hemispherically blunted body with a variable-depth streamwise nose cavity is considered in a Mach 5 airflow.

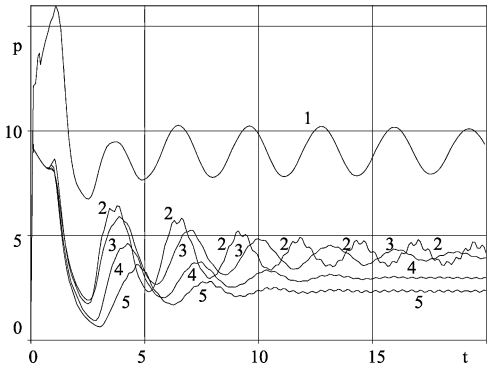

Fig. 6 Pressure variation in the center of the cavity bottom: 1, without energy deposition, 2, $W_0 = 20, f = 2.5$, spherical thermal spot; 3, $W_0 = 20$, $f = 2.5$, ellipsoid thermal spot; 4, $W_0 = 40, f = 2.5$, ellipsoid thermal spot; and 5, $W_0 = 80, f = 2.5$, ellipsoid thermal spot.

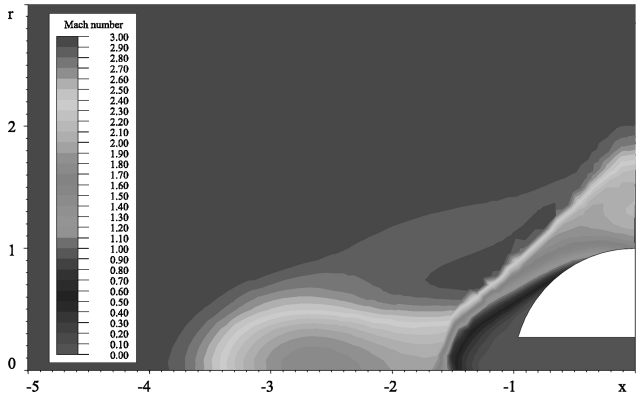

Fig. 7 Mach-number isolines for forward-facing cavity sphere.

The fluctuations for deeper cavities ($l_{\text{cav}}/R > 1.4$) become nearly sinusoidal in the experiments.[4]

Figure 7 shows the flow visualization near the sphere with the influence of the pulsating thermal source. The considerable increase of the bow shock standoff and the formation of recirculation zones in the shock layer correspond well with the data of Ref. 12. Thermal wake formations behind the energy deposition region lead to a reduction in gas density. The flow behind the energy deposition region remains supersonic (experimentally[12] verified).

The time-averaged drag coefficient was computed from the flowfiled data by using Eq. (14):

$$C = \frac{1}{T}\int_{t.-T}^{t.} C_x \, \mathrm{d}t \tag{14}$$

where $T = 10/f$ and C_x is the instantaneous drag coefficient defined by Eq. (15):

$$C_x(t) = \frac{4}{\gamma M_\infty^2}\int_0^1 (\gamma p_s - 1) r \, \mathrm{d}r \tag{15}$$

Figure 8 shows the ratio of the drag coefficient for the pulsed energy deposition to the drag coefficient without energy deposition. Similar to the case of hemispherical flow (no cavity),[13] a minimum of the cavity hemisphere drag coefficient is observed at the frequency change about $f \approx 2$ (Fig. 8). The effect of the parameter W_0 on the drag behavior was more significant as compare the influence of the thermal spot shape (Fig. 8) ($C/C_0 \approx 0.58$, $W_0 = 40$, ellipsoidal thermal spot; $C/C_0 \approx 0.59$, $W_0 = 20$, spherical thermal spot; $C/C_0 \approx 0.75$, $W_0 = 20$, ellipsoidal thermal spot; C_0 is the body drag without the energy supply). Further increasing W_0 results in the drag coefficient approaching as asymptote ($C/C_0 \approx 0.28$ takes place for the ellipsoidal spot at $f = 2.5$ and $W_0 = 500$, Fig. 9).

The cavity pressure pulsation magnitude is defined by both thermal spot dimensions and W_0. One can see (Fig. 6, curves 2–5) that

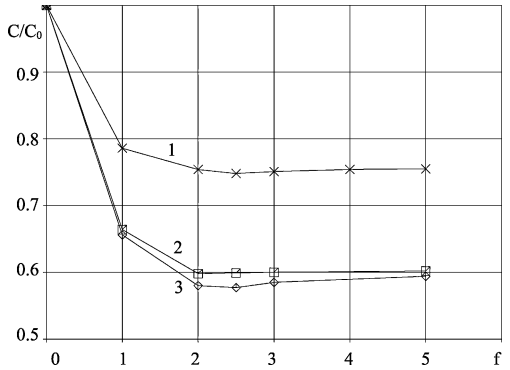

Fig. 8 Dependence of the drag coefficient C/C_0 with frequency changes f: 1, $W_0 = 20$, ellipsoid thermal spot; 2, $W_0 = 20$, spherical thermal spot; 3, $W_0 = 40$, ellipsoid thermal spot.

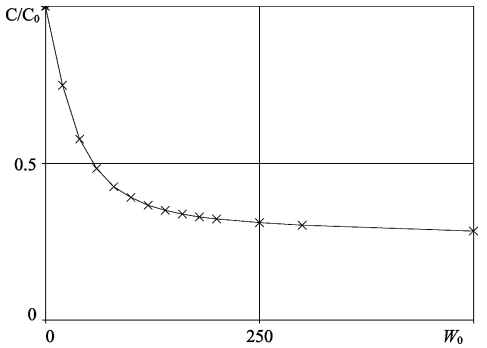

Fig. 9 Drag coefficient dependence on the parameter W_0: ellipsoidal thermal, $f = 2.5$.

transition from the spherical spot (curve 2) to the ellipsoidal one (curve 3) for the same parameter $W_0 = 20$ leads to larger attenuation of the pressure fluctuation in the cavity. When $W_0 = 40$ for the ellipsoidal spot (curve 4), one can observe a minimum pulsation amplitude pressure in the quasi-periodic state. Further increasing W_0 (curve 5) with stronger pressure pulsation attenuation leads to a rise in the pressure pulsation amplitude in the quasiperiodic state.

Conclusions

Our numerical simulation results in the following conclusions:

1) Thermal wake formation with nonuniform parameter distribution in the supersonic flow greatly influences the flow structure and the aerodynamic body drag.

2) Thermal spot configuration and power supply intensity define the magnitude of the pressure pulsation amplitude in the cavity.

3) A saturation effect is observed. This is based on our observation that the pulsation amplitude is not reduced ($W_0 = 40$, ellipsoidal thermal spot) for certain values of the W_0 parameter.

4) The drag coefficient change approaches an asymptote when the magnitude of the energy deposition increases.

5) Our results indicate that a pulsating heat source can be used as an effective method for supersonic spacecraft flow control.

References

[1]Huebner, L. D., and Utreja, L. R., "Mach 10 Bow-Shock Behavior of a Forward-Facing Nose Cavity," *Journal of Spacecraft and Rockets*, Vol. 30, No. 3, 1993, pp. 291–297.

[2]Yuceil, K. B., and Dolling, D. S.,"Nose Cavity Effects on Blunt Body Pressure and Temperatures at Mach 5," *Journal of Thermophysics and Heat Transfer*, Vol. 9, No. 4, 1995, pp. 612–619.

[3]Shui, V., Reeves, B., and Thyson, N., "Multiple Aperture Window and Seeker Concepts for Endo KEW Applications," AIAA Paper 92-2806, May 1992.

[4]Engblom, W. A.,Yuceil, B., Goldstein, D. B., and Dolling, D. S., "Experimental and Numerical Study of Hypersonic Forward-Facing Cavity Flow," *Journal of Spacecraft and Rockets*, Vol. 33, No. 3, 1996, pp. 353–359.

[5]Sambamurthi, J. K., Huernbner, L. P., and Utreja, L. R., "Hypersonic Flow over a Cone with a Nose Cavity," AIAA Paper 87-1193, 1987.

[6]Yang, H. Q., and Antonison, M., "Unsteady Flow Field over a Forward-Looking Endoatmospheric Hit-to-Kill Interceptor," *Journal of Spacecraft and Rockets*, Vol. 32, No. 3, 1995, pp. 440–444.

[7]Antonov, A. N., and Shalaev, S. P., "Experimental Investigation of Nonsteady Flow in Recesses in a Supersonic Flow," *Izvestya Academii.Nauk USSR, Mekhanika Zhidkosti i Gaza*, No. 5, 1979, pp. 180–183 (in Russian).

[8]Laoodon, D. W., Schneider, S. P., and Schmisseur, J. D., "Physics of Resonance in a Supersonic Forward-Facing Cavity," *Journal of Spacecraft and Rockets*, Vol. 35, No. 5, 1998, pp. 626–632.

[9]Bazyma, L. A., "Interaction Between Axial and Annular Jets Leaving a Cylindrical Cavity and an Incoming Supersonic Gas Flow," *Journal of Applied Mechanics and Technical Physics*, Vol. 36, No. 3, 1995, pp. 381–384 (translated from *Pricladnaya Mekhanika i Tekhnicheskaya Phyzica*, Vol. 36, No. 3, 1995, pp. 69–73).

[10]Utreja, L. R., and Gurley, W. H., "Aircraft Hollow Nose Cone," U.S. Patent 4,850,275 BDM International, Huntsville, AL, July 1989.

[11]Tret'yakov, P. K., Grachev, G. N., Ivanchenko, A. I., Krainev, V. L., Ponomarenko, A. G., and Tishenko, V. N., "Optical Breakdown Stabilization in the Supersonic Argon Flow," *Physics-Doclady*, Vol. 39, No. 6, 1994, pp. 415, 416 (translated from *Doklady Akademii Nauk*, Vol. 336, No. 4, 1994, pp. 446, 447).

[12]Tret'yakov, P. K., Garanin, A. F, Grachev, G. N., Krainev, V. L., Ponomarenko, A. G., Tishenko, V. N., and Yakovlev, V. I., "Control of Supersonic Flow Around Bodies by Means of High-Power Recurrent Optical Breakdown," *Physics-Doclady*, Vol. 41, No. 11, 1996, pp. 566, 567 (translated from *Doklady Akademii Nauk*, Vol. 351, No. 3, 1996, pp. 339, 340).

[13]Guvernyuk, S. V., and Samoilov, A. B., "Control of Supersonic Flow Around Bodies by Means of a Pulsed Heat Source," *Technical Physics Letters*, Vol. 23, No. 5, 1997, pp. 333–336 (translated from *Pis'ma v Zhurnal Tekhnicheskoi Fiziki*, Vol. 23, No. 9, 1997, pp. 1–8).

[14]Chakravarthy, S. R., and Osher, S. A., "New Class of High Accuracy TVD Schemes for Hyperbolic Conservation Laws," AIAA Paper 85-0363, 1985.

[15]Chakravarthy, S. R., "The Versality and Reliability of Euler Solvers Based on High-Accuracy TVD Formulations," AIAA Paper 86-0243, 1986.

[16]Georgievskii, P. Yu., and Levin, B. A., "Supersonic Flow Around Bodies in the Presence of External Heat Pulsed Sources," *Technical Physics Letters*, Vol. 14, No. 8, 1988, pp. 684–687 (in Russian).

[17]Godunov, S. K. (ed.), *Numerical Solution of Multidimensional Problems in Gas Dynamics*, Nauka, Moscow, 1976 (in Russian).

[18]Bazyma, L. A., and Kholyavko, V. I., "A Modification of Godunov's Finite Difference Scheme on a Mobile Grid," *Computational Mathematics and Mathematical Physics*, Vol. 36, No. 4, 1996, pp. 525–532 (translated from *Zhurnal Vychislitelnoy Mathemetiki I Mathematicheskoy Fiziki*, Vol. 136, No. 4, 1996, pp. 124–133).

P. Weinacht
Associate Editor